LARGE GRAVITATIONAL ROCK SLOPE DEFORMATION IN ROMSDALEN VALLEY (WESTERN NORWAY)

Aline SAINTOT[1, 2,*], Thierry OPPIKOFER[1], Marc-Henri DERRON[3] and Iain HENDERSON[1]

[1]Geological Survey of Norway (NGU), Postbox 6315 Sluppen, 7491 Trondheim, Norway
[2]Department of Endogenous Geology, Ruhr University Bochum, Universitätsstr. 150, 44780 Bochum, Germany
[3]Institute of Geomatics and Risk Analysis, University of Lausanne, Amphipôle, 1015 Lausanne, Switzerland
[(*)]Corresponding author: aline.saintot@rub.de

ABSTRACT

Large gravitational rock slope deformation affects Precambrian gneisses at four localities of the Romsdalen valley of Western Norway. At each locality, detailed studies have allowed to determine the mechanism of deformation and to assess the degree of susceptibility for failure. 1) Svarttinden is a 4.3 Mm^3 translational rockslide. Its single basal detachment developed along a foliation-parallel cataclastic fault. Although a rockslide occurred along the same detachment and the deposits reached the edge of the plateau, no displacement of the current instability is detected. 2) At Flatmark distinct 2-25 Mm^3 blocks detached from the edge of the plateau by an opening along the steep foliation. The collapse of the blocks is explained by a complex mechanism of sliding and toppling. No displacement is actually detected on the instabilities. 3) At Børa blocks located at the edge of the plateau deformed by the same mechanism as at Flatmark. They have a maximum volume of 0.5 Mm^3 and displacement rates of 0.2-2 cm/year. The deformation at Børa has affected a large part of the plateau and the entire deformed volume would be of 50-200 Mm^3 but it is currently inactive. 4) A wedge failure at the edge of Mannen plateau is inferred to allow the 4-5 cm/year downward displacement of a 2-3.5 Mm^3 instability. The high susceptibility of failure led to a permanent monitoring of the site since 2009.

Keywords: *rockslide, structural analysis, mechanism.*

RESUMEN

Deformación gravitacional de las vertientes rocosas del valle de Romsdalen (Noruega occidental).
Una gran deformación gravitacional afecta unidades gnéisicas precámbricas en cuatro localidades del valle Romsdalen, Oeste de Noruega. En cada localidad, estudios detallados permitieron determinar el mecanismo de deformación y evaluar el grado de susceptibilidad al colapso. 1) Svarttinden es un deslizamiento translacional de 4.3 Mm^3. Su plano basal se desarrolló a lo largo de una falla paralela a planos con deformación cataclástica. Si bien un deslizamiento tuvo lugar a lo largo del mismo plano basal, y los depósitos alcanzaron el borde del *plateau*, no se detecta desplazamiento en la zona inestable. 2) En Flatmark, bloques de 2-25Mm^3 se desprendieron del borde de la meseta a partir de la apertura de planos de foliación de gran inclinación. El colapso de bloques es explicado por un complejo mecanismo de deslizamiento y volcamiento. No se detecta actualmente desplazamiento en las zonas inestables. 3) En Børa, bloques ubicados en el borde de la meseta fueron deformados por el mismo mecanismo que en Flatmark. Los mismos tienen un volumen máximo de 0.5 Mm^3 y tasas de desplazamiento de 0.2-2 cm/a. La deformación en Børa ha afectado gran parte de la meseta y el total del volumen deformado sería de 50-200 Mm^3, si bien se encuentra actualmente inactiva. 4) Un colapso en cuña en el borde de la meseta Mannen permitiría un desplazamiento de 4-5 cm/a pendiente abajo, de 2-3.5 Mm^3. La alta susceptibilidad al colapso, dio lugar a un monitoreo permanente del sitio desde el año 2009.

Palabras clave. *deslizamiento, análisis estructural, mecanismo.*

INTRODUCTION

Western Norway is a region of important topographic gradient. Like in the Andes and other mountain regions in the world, the relief is prone to large rock slope failures. As the latter may have catastrophic consequences in terms of life loss, the Norwegian government launched a long term program to map and study the sites of large gravitational rock slope deformation. The large instabilities that directly endanger the community are under investigation for detection of displacements. Aside, geological investigations for a better understanding of the major features that control these instabilities are carried out. This is the case for the four large gravitational rock slope instabilities at Svarttinden, Flatmark, Børa and Mannen, in Romsdalen valley for which the susceptibility for failure has to be accurately determined (Figs. 1 and 2). Hence, multi-disciplinary studies of these instabilities are carried out for approximately 10 years and rock slope displacements are detected at Børa and Mannen.

The 30 km long Romsdalen valley is an over-deepened U-shaped glacial valley, typical of the extreme alpine relief of Western Norway (Etzelmüller *et al.* 2007; Fig. 1). It is characterized by the highest spatial density of past, including historical, rock slope failures in Norway. The present contribution focuses on the structural development of the four instabilities with the principal aim of understanding the failure mechanism. All four developed on the southern slope of the valley in a suite of intensively tectonized high-grade metamorphic Precambrian gneisses. Studies of large rock slope instabilities in similar intrinsically strong rocks have demonstrated the quasi-systematic reactivation of inherited structures in the gravity-driven deformation and large volumes of these types of rocks effectively destabilize where the pre-existing structures favorably dip relatively to the slope (e.g. Cruden 1976, Mahr 1977, Varnes 1978, Giraud *et al.* 1990, Guzzetti *et al.* 1996, Julian and Anthony 1996, Sauchyn *et al.* 1998, Hermanns and Strecker 1999, Agliardi *et al.* 2001, Kellogg 2001, Eberhardt *et al.* 2004, Brideau *et al.* 2005, 2009, El Bedoui *et al.* 2008, Jaboyedoff *et al.* 2009, Welkner *et al.* 2010). The same conclusion is drawn from extensive studies on the development of large rock slope instabilities over Western Norway with, in many cases, the metamorphic foliation accommodating a prominent part of the deformation (e.g. Braathen *et al.* 2004, Henderson *et al.* 2006, Ganerød *et al.* 2008, Oppikofer 2009, Böhme *et al.* 2011, Jaboyedoff *et al.* 2011; Oppikofer *et al.* 2011, Saintot *et al.* 2011b). Field studies (Henderson and Saintot 2007) combined with the inspection of aerial photographs and analyses of meter-scale resolution Digital Elevation Model (DEM) from airborne laser scanning (ALS) and terrestrial laser scanning (TLS; see in Oppikofer *et al.* (2012, this volume) for an exhaustive description of the latter) result in detailed structural maps and dataset collections, which allow us to determine the type of slope deformation as well as to assess the kinematics of the potential failure at each site. With the help of independent data (occurrence of previous failures, monitoring of displacement by differential Global Positioning System (dGPS), etc.) a qualitative assessment of the susceptibility for failure is attempted. The term "susceptibility for failure" is used here instead for "hazard", because for the investigated rock slope instabilities there are no temporal constraints on the likelihood of failure, which according to Fell *et al.* (2008) are necessary for a thorough "hazard" assessment.

REGIONAL BEDROCK AND QUATERNARY GEOLOGY

Romsdal valley cuts into the crystalline basement of the Western Gneiss Region of Norway. The bedrock belongs to the severely deformed and tectonized Precambrian autochthon (or para-autochthon) of the Caledonides (Roberts and Gee 1985). Three geological basement units are identified along the Romsdalen valley by Tveten *et al.* (1998). Most of the area is covered by the typical, and probably the oldest, granitic to dioritic gneiss unit of the basement (Fig. 2). The instabilities at Svarttinden, Flatmark and Børa developed in this unit. A lens of coarse-grained granitic and augen gneisses of meso- and neo-Proterozoic ages (1600-542 Ma) crops out north-east of the studied area (Fig. 2). A widespread unit consists of a quartz-rich gneiss unit characterized by sillimanite and kyanite of uncertain ages spanning from Proterozoic to Paleozoic. The instability at Mannen developed in this unit.

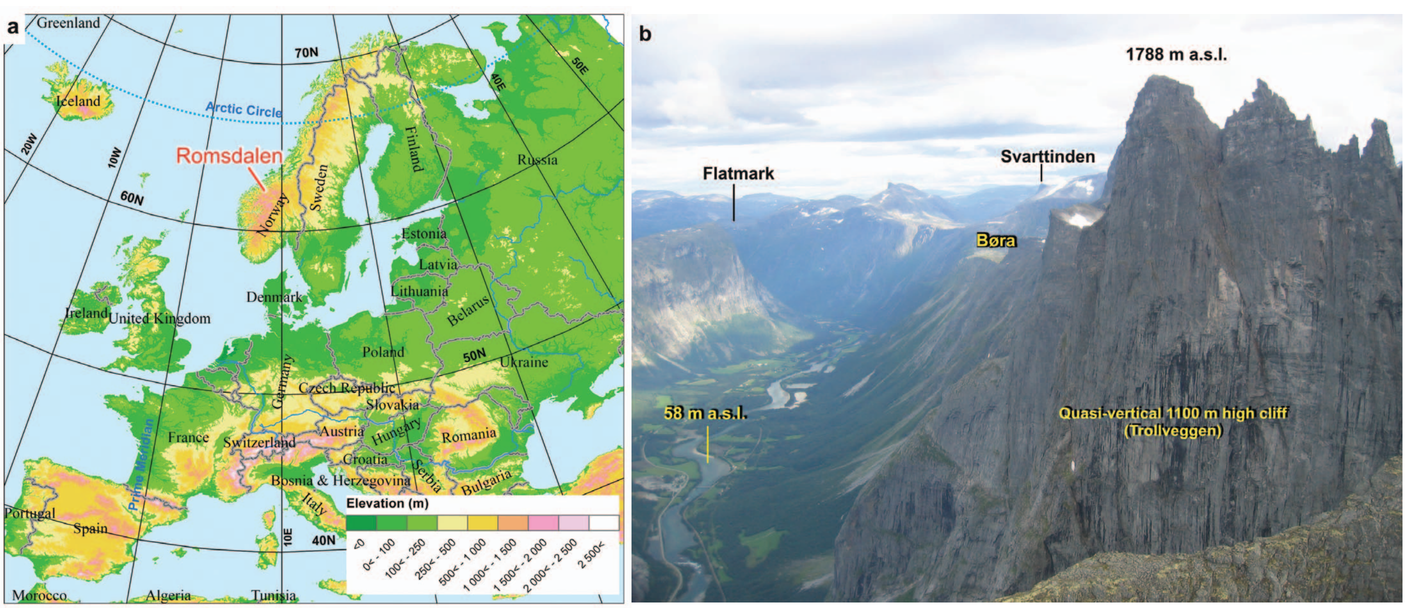

Figure 1. a) Topographic map of Europe with Norway showing an Alpine relief and location of Romsdalen valley. b) View of Romsdalen to the east displaying the typical U-shape of the over-deepened glacial valley (Børa, Svarttinden and Flatmark are three of the unstable slopes described in the present contribution).

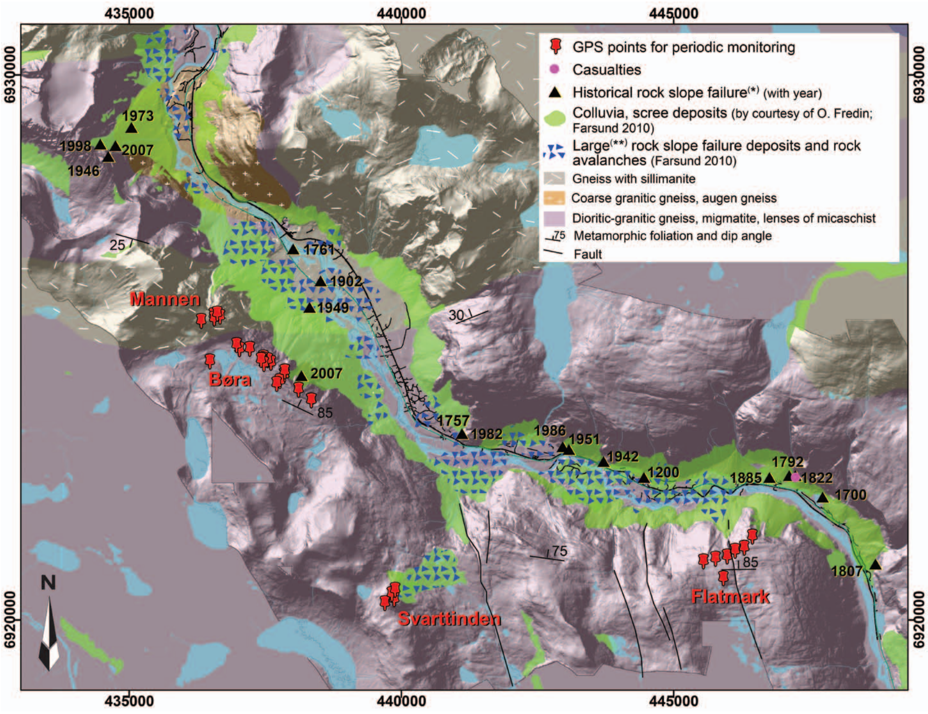

Figure 2. Geological map of Romsdalen (from Tveten *et al.* 1998) on a hillshaded ALS-DEM (coordinates in UTM zone 32). Romsdalen is characterized by the highest density of past and historical rock slope failures in Western Norway and by four current large gravitational rock slope instabilities: Flatmark, Svarttinden, Børa and Mannen. (*), either placed at the source areas or at the deposits (Dahle *et al.* 2008, Skrednett 2012), (**), > 100 000 m^3.

After the Caledonian Orogeny, the basement of the Western Gneiss region significantly exhumed during the Devonian collapse of the chain (Hossack and Cooper 1986; Roberts 2003). The age of the major brittle structures observed on Romsdalen valley (Fig. 2) is not constrained. They can pertain to this Devonian tectonic phase as well as to other brittle tectonic phases that are known to have affected the Western Gneiss Region (i.e. for the most significant, the Permo-Trias and Jurassic rifting episodes; Torsvik *et al.* 1997, Valle *et al.* 2002, Mosar 2003). The (still ongoing) uplift of the basement started at a debated time. Anyway, the drainage river system was surely installed during the Tertiary and already shaped the present-day landscape.

The Quaternary geology of the region is marked by glaciation episodes. The ice extended to the outer part of the continental shelf during the maximum of the last glaciation in the Weichselian (Mangerud 2004). During the Younger Dryas last severe cooling event, the glaciers re-advanced close to the coast and frost wedging into preexisting fractures is thought to have been a primary factor of rock slope instability development (Blikra *et al.* 2006).

The ice cap melting generates a regional isostatic rebound and large-magnitude earthquakes (Olesen *et al.* 2000, 2004). Combined with the sudden unloading of the steep slopes due to the rapid glacier retreat an important amount of large rock slope failures occurred shortly (1000 to 2000 years) after the deglaciation (Blikra *et al.* 2002, 2006, Longva *et al.* 2009).

The work of glaciers enhanced the relief to produce the spectacular landscape (fjords, cirques, lakes) of Western Norway and the typical U-shaped Romsdalen valley was carved by the retreated glaciers. Moraines and tills of the last Younger Dryas ice sheet are conspicuous in Romsdalen valley that was probably free of ice some 10 000 years ago or so (Mangerud 2004). No rock slope failure deposits linked to the ice debuttressing of the slopes are preserved in Romsdalen valley bottom. If rock slope failures occurred at that time, the associated deposits were likely far transported by the remnant glacier and/or covered by deltaic and marine fine-sand, silt and clay deposits that filled the valley in postglacial Holocene times.

More than 15 rock avalanche deposits (larger than 100 000 m^3) are mapped in the 30 km long Romsdalen valley (Fig. 2, Blikra *et al.* 2006, Farsund 2010) and are therefore the most recent significant infill of the valley bottom. This is among the highest concentrations of rock avalanches on land in Norway (Blikra *et al.* 2002). They occurred during the last 5,000 years (Blikra *et al.* 2006). Charcoal below one of these rock avalanche deposits yielded an age younger than 2,000 years BP (Blikra *et al.* 2006). Nineteen historical rock slope failures (Skrednett 2012; Dahle *et al.* 2008) are recorded over the study area of Romsdalen valley (Fig. 2).

METHODS

Structural analysis and kinematic feasibility tests

To assess the kinematic (geometric) feasibility of failure of rock slope instability, a detailed structural analysis is performed. The main different kinematic models of rock slope failure are toppling, planar sliding and wedge sliding (e.g. Varnes 1978, Hoek and Bray 1981, Cruden and Varnes 1996, Braathen *et al.* 2004). Most of the large rock slope instabilities in the hard gneissic rocks of Western Norway deformed by planar or wedge sliding (Braathen *et al.* 2004, Henderson *et al.* 2006, Oppikofer 2009, Henderson and Saintot 2011, Oppikofer *et al.* 2011, Saintot *et al.* 2011b). It is also well known that in hard gneissic rocks the gravitational deformation reactivates the pre-existing structures of the rock mass. Therefore, the structural analysis at a site consists to collect the different sets of preexisting discontinuities in the aim to identify the ones which may accommodate the gravitational deformation (that lead to the development of the instability). The collection of discontinuity sets is a priority during fieldwork. However, due to the steepness of the slopes, measurements are often spatially restricted to few zones of the entire instability.

ALS and TLS data and derived DEM permit to measure the orientation of discontinuities of large parts of the instability (e.g. Jaboyedoff *et al.* 2009, Oppikofer *et al.*

2009, 2011, Pedrazzini *et al.* in press). The assumption is that the topographic surfaces of steep rock slopes are shaped by the major fracture surfaces in the rock mass. Therefore, the orientation of these fractures can be extracted from the local orientation of the topographic surface. Here we use two raster models, slope aspect and slope angle, calculated from the ALS-DEM in ArcGIS® system (ESRI 2010). The values of the slope aspect and of the slope angle for the same DEM cell give the full orientation (dip direction and dip angle) of the topographic surface and hence of the rock discontinuity. The high resolution of the ALS-DEM (1 m cell size), which is available in the Romsdalen valley, ensures an accurate measurement of the fracture orientations. Selecting regions with homogeneous orientation allows computing the mean orientations of the discontinuities of the rock mass, which in turn leads to distinguish the sets that mechanically account for the failure and to define the mode of failure.

Volume estimation

The preferred method to accurately define the volume of the rock slope instability is to compute the differences between the present topography and the supposed basal failure surface (Jaboyedoff *et al.* 2004a, b, Oppikofer 2009, Oppikofer *et al.* 2012, this volume). Therefore, the goodness of the volume estimation of the rock slope instability depends of the degree of knowledge of its geometry, i.e. of the spatial extent in 3D of the basal failure surface. In many cases, it is difficult to estimate the depth of deformation even though the gravitational deformation can be well delimited on a map (in 2D). For example, the rough estimation of the volumes of the instabilities at Børa is due to the uncertainty in the depth of deformation, i.e. the accurate determination of the basal failure surface. In turn, the basal failure surface of Svarttinden rock slide crops out and an accurate calculation of the volume can be performed. In such cases, a 3D model of the possible failure surface is built in the software PolyWorks® (InnovMetric 2012) by following the present morphology in the surroundings of the rock slope instability and extending the observed structures underneath the instability (Oppikofer 2009). With the analysis of the high-resolution DEM of Romsdalen, the location of potential basal surfaces may be recognized by geomorphological signs on the slope where the surfaces should daylight. The latter are somehow well displayed at Mannen and moreover the proposed failure surfaces fit with zones of severe deformation observed along a core drilled from the top of the instability. At Flatmark, the geomorphological signatures of the structures on which may accommodate the deformation at the base of the instabilities are not enough pronounced on the slope to ascertain their location. It results a rough estimation of the unstable volumes.

SVARTTINDEN

Svarttinden is a 1600 m altitude mount, located at 1.2 km inward the plateau from the cliff (Fig. 2). The whole mount is a translational rockslide lying on a single moderately NE-dipping basal detachment (Figs. 3 and 4, Henderson and Saintot 2007).

A large volume already failed from the eastern part of the basal detachment and the deposits reached the edge of the plateau but not the valley floor. Rock avalanche deposits in the valley likely originated from scars at the edge of the plateau (Fig. 3). Smaller failures from the three free faces of the remaining instability followed and the relat-

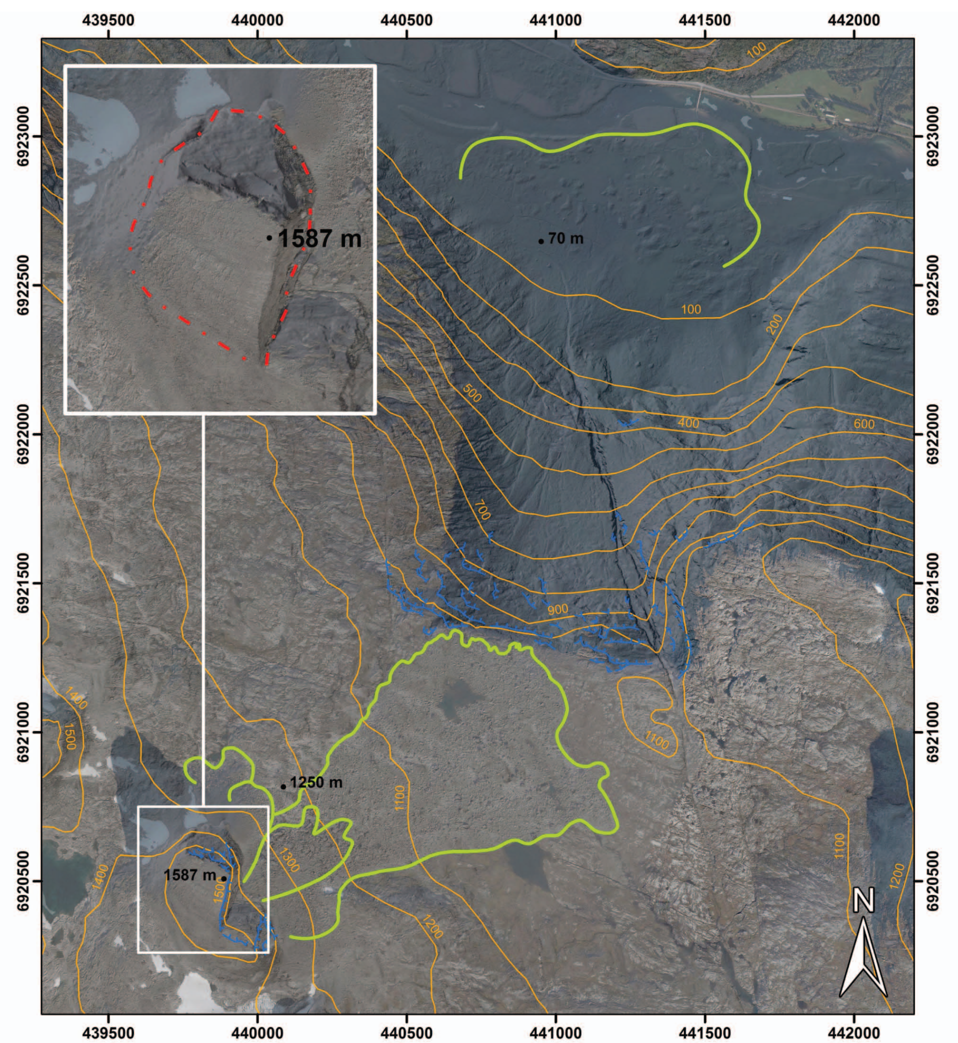

Figure 3. Svarttinden: a large remaining rock slope instability west of a previous failed slope (in white frame). Blue lines: scars of previous rock slope failures; green lines: limits of deposits of previous failures; red dashed line: trace of the single basal detachment of the translational rockslide.

ed deposits are clearly superimposed on the large deposit of the previously failed eastern volume (Fig. 3).

The background fracturation of the gneiss corresponds to steep-to-vertical NW-SE and NE-SW/NNE-SSW trending sets and foliation-parallel sets (Fig. 4). The foliation is moderately to steeply dipping to the NE and NNE. The foliation steepens toward the frontal part of the instability (Fig. 4). A prominent NNE-SSW steep planar fracture forms the border between the failed slope and the remaining block (Fig. 5a). The basal detachment crops out well due to the previous failure east of the rockslide and can be plainly characterized (Figs. 4 and 5). It developed along a metamorphic foliation surface. Its surface is rough and displays meter-scale amplitude undulation which corresponds to the ductile fabric of the foliation (Fig. 5a, b). It is also stepped by rupture along the NW-SE steep joints (Figs. 4 and 5).

Field observations result in the assumption that sliding of the instability has occurred. On the eastern side of the block, tensile minor structures in the hanging wall of the basal detachment and a 20 cm thick layer of silty-grained unconsolidated breccia observed along the detachment are both inferred to be the products of the gravity-driven displacement of the block (Henderson and Saintot 2007; Fig. 5c, d). On the western side of the block, gravitational deformation is expressed by large cracks which vertically developed from the top surface of the block and parallelized downward to the valley-dipping metamorphic foliation (Henderson and Saintot 2007; Fig. 6a). Cavities are also visible and elongated along the basal detachment. They may either be due to an offset along the undulated basal detachment or to the removal of uncemented breccia material from lenses

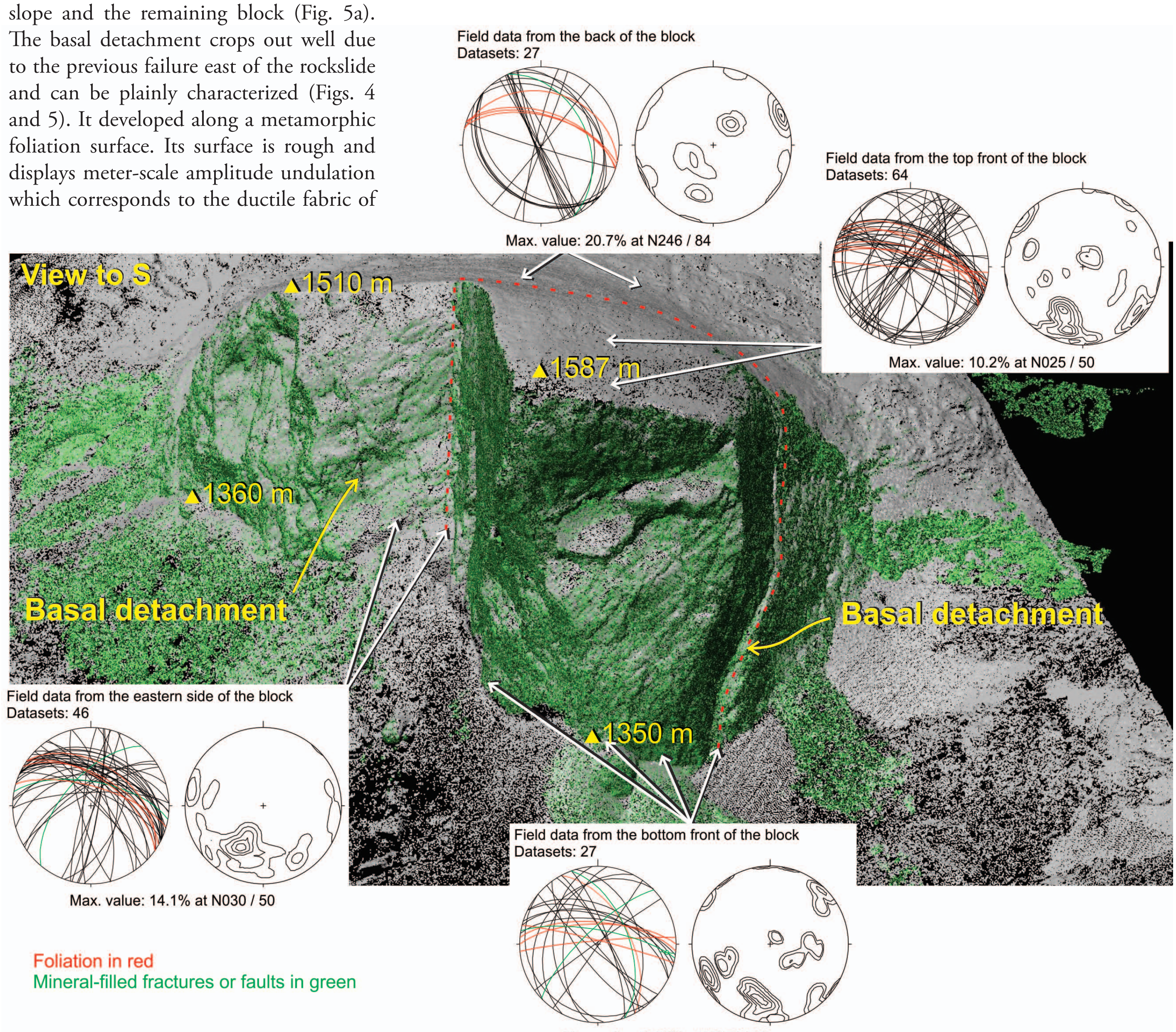

Figure 4. Stereoplot of structural field measurements at locations shown on a 3D view of Svarttinden. The green dots are the TLS point cloud superimposed on the hill-shaded ALS-DEM in gray; the red dashed line is the trace of the single basal detachment of the translational rockslide.

(Fig. 6a, b). The current rockfall source areas are the western and eastern steep sides of the instability as well as the hinges of recumbent tight folds of the northern face (Figs. 5a, b and 6a, b).

The basal detachment developed along an ancient ductile shear zone as indicated by the deflection of the foliation to become parallel to it (Fig. 6a). This zone was the locus of a later tectonic reactivation in the brittle regime to become a chlorite- and epidote-coated cataclastic fault zone (Fig. 6c). Hence, the gravity-driven deformation occurred along a brittle fault zone that has likely developed along a pre-existing ductile shear zone. The observation at Svarttinden gives further support to the hypothesis that the gravitational structures in hard gneissic rocks commonly develop on distinct weak zones created by tectonic forces.

The mean orientation of the basal detachment was extracted from the numerical topographic surface orientation (slope gradient and direction derived from a 1 m resolution DEM) and is of 44° to N034 and of 46° to N048, east and west of the block respectively (Fig. 7). These two orientations are confirmed by scattered field measurements on the outcropping basal detachment, east and west of the current instability (Fig. 4). These are mean orientations and the 3D view of Svarttinden indeed displays the undulations of the basal detachment and specifically of its western outcropping part which steepens and rotates toward the front of the block to be ENE-directed (Fig. 4). Nevertheless, the fitting of the eastern and western outcropping parts of the basal detachment identified on the DEM resulted in a similar mean orientation with a plane dipping 50° to N040. This good morphologic and structural control of the basal failure surface made the Svarttinden instability propitious for 3D modeling and volume estimation. Using a single plane as basal failure surface yields a volume of 4.3 Mm^3 for the remaining rock slope instability. The volume that failed east of the instability was probably of the same order or less.

The Svarttinden rockslide is monitored by dGPS since 2006 because of the occurrence of (1) a well-developed basal sliding surface, with locally the occurrence of a fine-grained breccia lowering the friction, (2) a previous failure of similar size along the same surface and (3) rockfall activity from the remaining block. However, the rockfall activity may be simply due to the steepness of the faces of the block rather than induced by motion of the block. Indeed, no significant displacement of the rockslide is detected until now. This is in agreement with the field survey at the back of the block, which reveals that no conspicuous recent disturbance of the rocks is observed where the basal detachment intersects the topographic surface (see for example on the aerial photograph of Fig. 7). The high roughness and the undulations of this basal surface is a primary factor that may explain the absence of motion of the instability. A second factor may be the change of orientation of this surface. As mentioned above, its orientation is approximately of 45° dipping to the NE except at the bottom frontal part of the block where the surface steepens and shifts to an ENE dip direction. It cannot be ruled out that the change of orientation of the basal detachment toward the toe zone avoids it from day lighting the topography

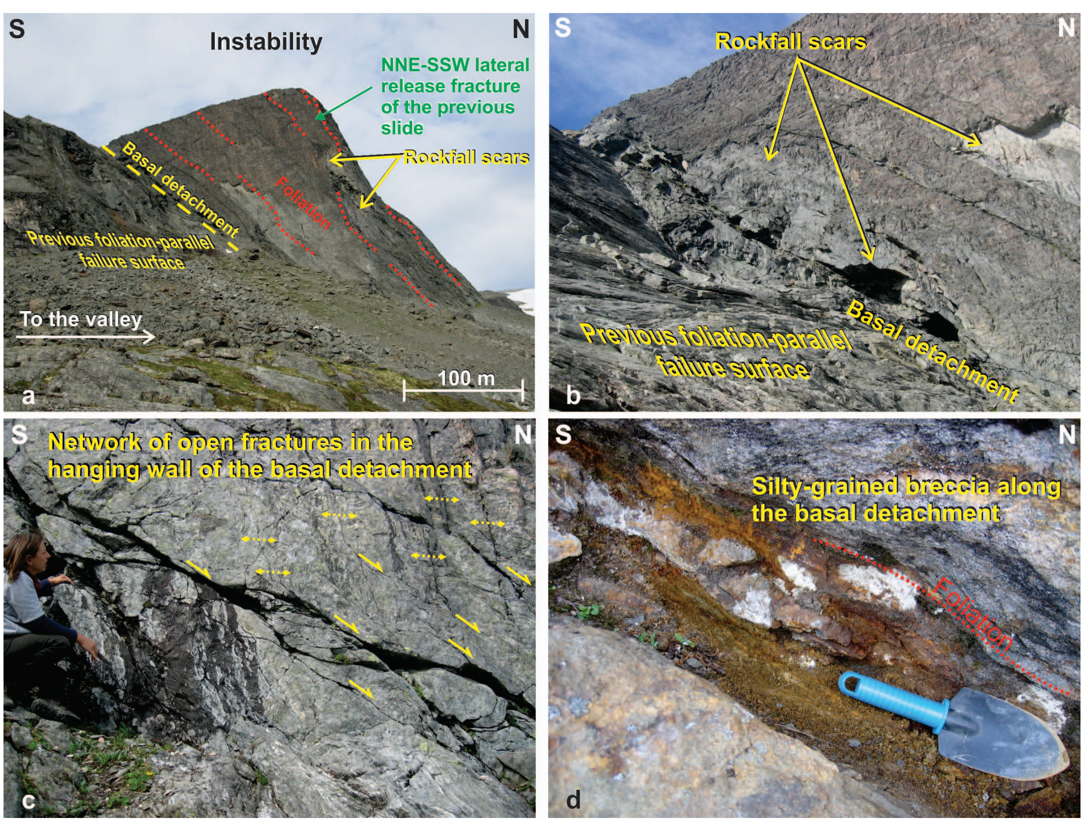

Figure 5.
Svarttinden: photographs of the eastern side of the current unstable block. a) View of the remaining instability over the basal detachment of the previous rock slope failure. b) Roughness of the basal detachment (undulation and steps) and rockfall activity from the remaining instability. c) Deformation in the hanging wall of the basal detachment interpreted to accommodate the gravity-driven displacement of the remaining instability. d) Unconsolidated breccia along the basal detachment interpreted to be the product of past displacements.

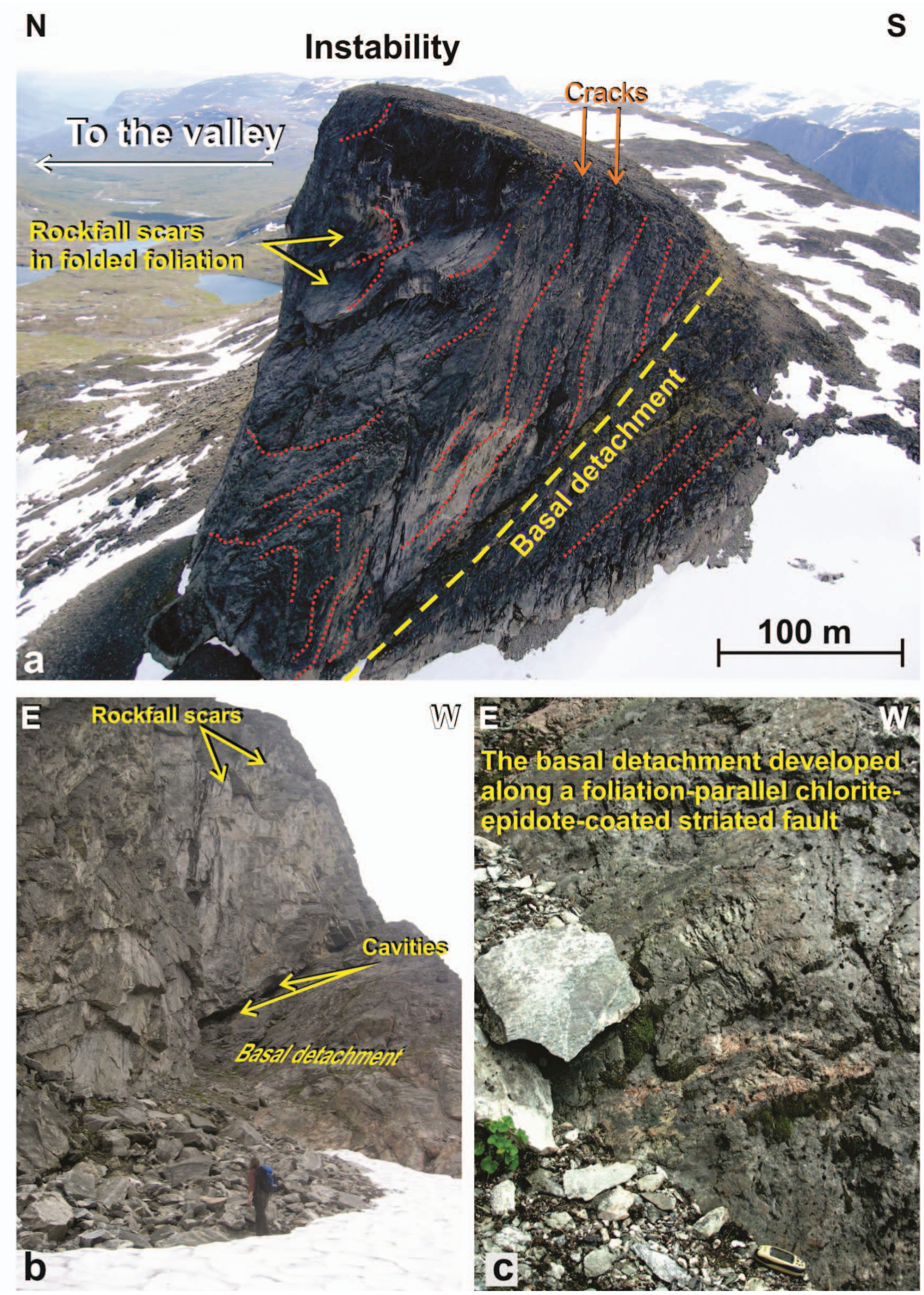

Figure 6. Svarttinden: photographs of the western side of the remaining instability. a) View from helicopter showing (1) the sources of rockfalls at the hinges of recumbent folds and (2) the ductile deformation of the metamorphic foliation and the pre-existing ductile shear along the present-day basal detachment. b) Rockfall activity from the remaining instability and elongated cavities along the detachment (seen also on (a)). c) The basal detachment of the rockslide is a pre-existing foliation-parallel chlorite- and epidote-coated cataclastic fault.

and thus acts against the sliding of the total block by a buttressing effect.

FLATMARK

At Flatmark (Fig. 2), a series of rock slope instabilities extends from the edge of the plateau at 900 to 1050 m a.s.l. to large parts of the slope downward (Fig. 8). A succession of rock avalanches and large rock slope failure deposits, including historical ones, are mapped on the valley floor at the bottom of Flatmark (Fig. 2). Flatmark is expected to be the source area of most of them.

The rock slope instabilities at Flatmark are delimited by wide vertical back-cracks that have partly smooth walls parallel to the quasi-vertical metamorphic foliation and partly stepped walls shaped by the same foliation and steep quasi-meridian joints (Fig. 8). For the uppermost and largest instability the width of the back-crack is 20–25 m. Only few opened fractures of small amplitude are observed inward the plateau at the back of the rock slope instabilities. This testifies of the important localization of the large gravitational deformation at the edge of the plateau (see also discussion in Böhme *et al.* 2011).

The structures that may represent the basal failure surfaces of the instabilities are not yet clearly identified, the fieldwork being unfortunately restricted to the plateau edges due to the steepness of the slope (Fig. 9). At the base of small surficial displaced blocks two favorably orientated, valley-dipping planes were collected (Fig. 9), which might represent a fracture set forming also a larger basal sliding surfaces at depth. However, the scarcity of field measurements questions about their real significance at the scale of the entire slope. Nonetheless, a set of joints can be observed that systematically developed perpendicular to the dip line of the metamorphic foliation (Fig. 8). The field study on the plateau has indeed permitted to observe the variation of the metamorphic foliation from quasi-vertical to clearly dipping toward the mountainside (Figs. 8g and 9). At the locations where the foliation dips into the slope, the joints that formed perpendicular to its dip line are so favorably orientated toward the valley that they may act as basal sliding surface. The sharp topographic surfaces of the slope downward the largest instability may actually reflect the foliation dipping into the mountain and moderately valley-dipping topographic surfaces would correspond to such a joint set (Fig. 8h).

The analysis of the topography (Fig. 10) tends to assign basal limits of the instabilities on shallow to moderately valley-dipping surfaces (Fig. 10b, c). The possible failure mechanism of the large rock slope instabilities at Flatmark is likely a sliding and/or a sagging on these valley-dipping basal failure surfaces yielding back-crack

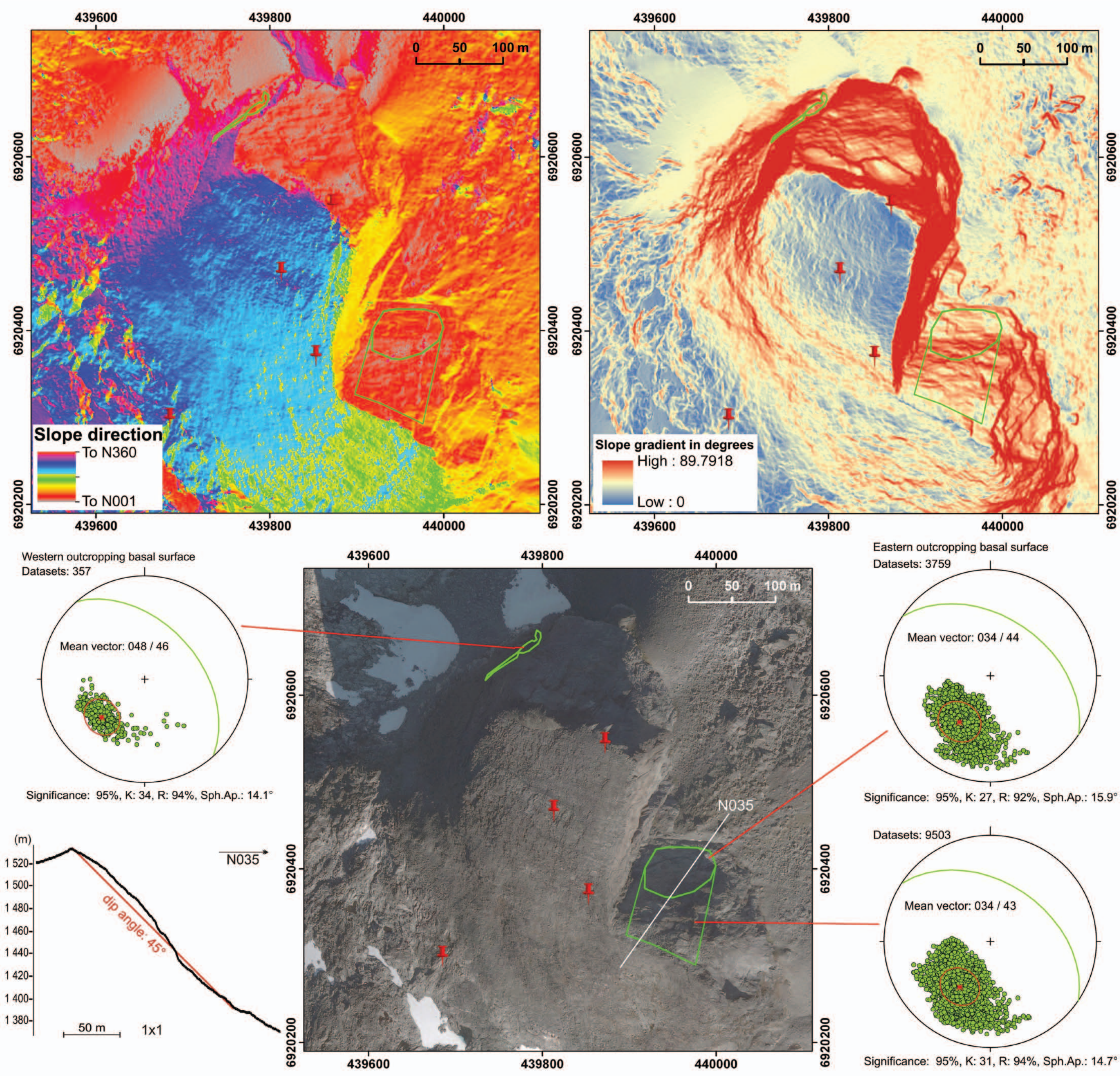

Figure 7. Top: maps of the slope direction (left) and gradient (right) derived from the ALS-DEM. Areas limited by green lines: western and eastern outcropping sides of the basal surface of the Svarttinden rockslide. Bottom: Stereoplots of the slope orientations of the western and eastern sides of the basal sliding surface (1 point per DEM cell). Slope profile directed to N035 across the eastern outcropping basal sliding surface (along which occurred the previous failure) and indicating an average dip angle of 45°; aerial photograph of Svarttinden rockslide with location of the profile. Note on the mean vector calculation: *Mean vector*, azimuth/plunge; *Significance (%)*, prediction probability of the cone of confidence; *K***,** concentration parameter (closeness, precession) after Fisher (1953) ranging between 2 (uniform distribution) and infinity (parallel fabrics); *R (%)*, concentration parameter from Wallbrecher (1986) ranging from 0% (uniform distribution) to 100% (parallel fabrics); *Spherical aperture (°)*, radius of a small circle of a spherical normal distribution with equal *R*-value as the given data.

opening along the cliff-parallel steep metamorphic foliation planes. Locally, a toppling mechanism clearly affects small pieces of rock at the top of the blocks (Fig. 8). However, the vertical extents of the back-cracks and the continuity of the basal failure surfaces are speculative and stepped surfaces cannot be ruled out (Fig. 10b). Nevertheless, one of the instabilities has by contrast well-defined borders that stick, eastward and westward, to a vertical N-S cataclastic fault and its east-dipping branch respectively, and follow, backward, an E-W vertical foliation plane (Fig. 9).

The total deformed volume would reach

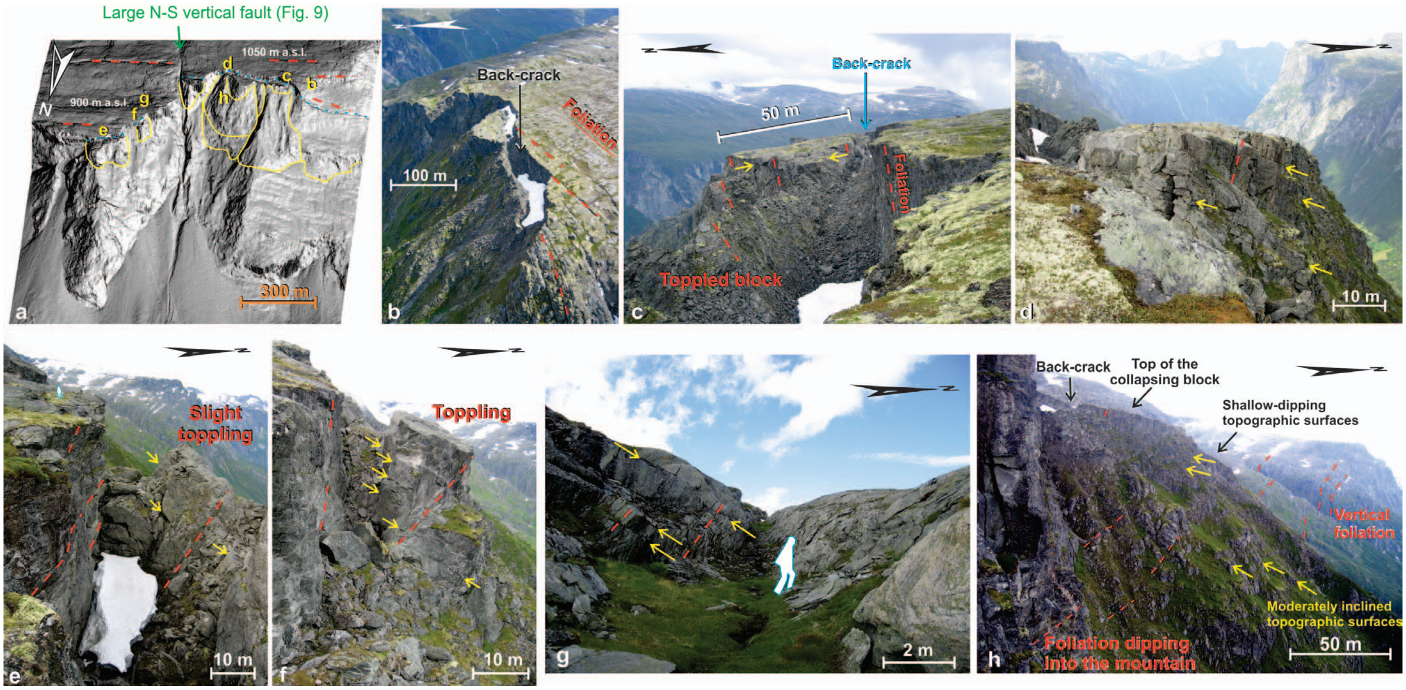

Figure 8. a) Flatmark: 3D view of the hillshaded ALS-DEM showing rock slope instabilities of various sizes (back-cracks at the edge of the plateau as blue dashed lines, limits of instabilities on the slope as yellow lines, traces of the steep metamorphic foliation as red dashed lines; locations of photos in (b) (h) are shown). b)h) photographs of the rock slope instabilities at Flatmark with the trace of the metamorphic foliation (red dashed lines) and shallow to moderately valley-dipping joints that developed perpendicular to the foliation dip line (yellow arrows). b) View from helicopter of the largest instability with a back-crack opening partly guided by a pre-existing quasi-vertical metamorphic foliation. c) close view to the east of the 20 m wide back-crack largely filled by debris; the instability is affected by toppling. d) Close view to the west of the largest instability. e) And f) toppling displacements observed at the top of two instabilities in the eastern part of the Flatmark plateau. g) Surface depression in the eastern part of the plateau. h) Shallow to moderately valley-dipping topographic surfaces on the largest rock slope instability corresponding to joints that systematically developed perpendicular to the foliation dip line; these are favorably orientated toward the valley where the foliation steeply dips into the mountain and where the basal sliding surfaces of the instabilities are expected to daylight.

155 Mm^3 with subsidiary blocks of volumes ranging between 2 and 25 Mm^3 (Henderson and Saintot 2007, Longchamp *et al.* 2010). Because of the large degree of deformation observed at Flatmark and because the site was the source area of large deposits lying on the valley floor (Fig. 10a), the unstable blocks are monitored since 2006 by dGPS measurements but no displacements are detected until now. This is in agreement with (1) the important infill of the back-cracks with deposits (Fig. 8a, b) and with (2) the absence of rockfall activity at the front of the deformed volumes as well as of well-developed bulges due to advancing slopes. The latter is confirmed by the regularity of the topography as displayed on profiles crossing the instabilities (Fig. 10b). A slight bulge might have nevertheless developed across the lowest unstable block which also shows the highest rate of rock dislocation (see topography along profile 5 on Fig. 10b, Fig. 8e).

BØRA

The geological and geomorphological settings at Børa (Fig. 11) are the same as at Flatmark with the exception of a large paleo-glacial perched valley at Børa trending parallel to the slope. Otherwise, both sites comprise identical gneissic rocks characterized by a steep to vertical foliation, shaping parts of the cliff at the edge of the plateau. Like at Flatmark, several rock slope instabilities developed along foliation-parallel back-cracks at the edge of the cliff at 1000 m altitude and are the sources of frequent rockfalls (Fig. 11a-c). At least 5 previous large rock slope failures occurred from the cliff of Børa including historical events (Fig. 2; Blikra *et al.* 2002). The last rockfall dates from 2007 and involved a significant volume of 30 000 to 50 000 m3 (Dahle *et al.* 2008) with deposits that reached the valley bottom.

Contrary to Flatmark where the severe gravitational deformation is restrained to blocks at the edge of the plateau, the gravity-driven deformation encompassed a large area at Børa, going well inward the plateau. The limit of the deformed rock slope is marked by a one kilometer long, several meters wide and deep, foliation-parallel, back-bounding crevasse. The crevasse is particularly well-developed in its eastern part (Fig. 11d) and dies out westward (Fig. 12) leading to a decrease in past deformations from east to west.

Two conspicuous sets of structures accommodate the gravitational deformation by opening and comprise the quasi-vertical WNW-ESE foliation and a vertical NNW-SSE fracture set (Fig. 12a, b). They both shape the edge of the plateau. A toppling mechanism along these two geometries is impossible given the importance of the deformed volume, and a third set of discontinuities may exist to limit the deformation at depth. The general background of dis-

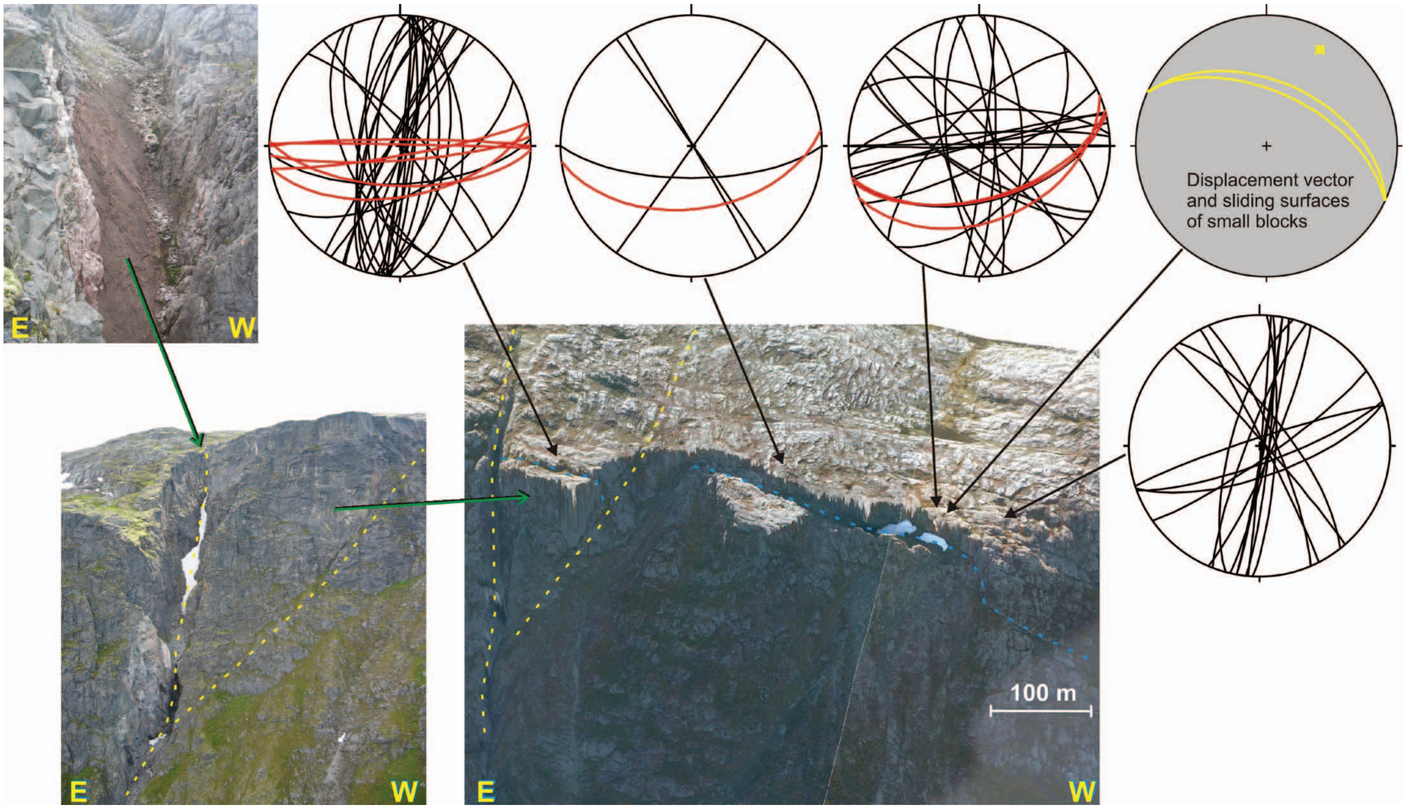

Figure 9. Stereoplots of field measurements at the edge of the Flatmark plateau where the largest instability developed: metamorphic foliation in red and joints in black, two planes at the base of small detached blocks have an orientation favorable for sliding. Locations of field measurements on a 3D view of the top of the largest instability (aerial photograph draped on DEM). Photographs taken from helicopter of one of the instabilities, delimited by a foliation-parallel back-crack (blue line) and two preexisting tectonic faults (yellow lines), one being largely hematite-rich cataclastic (located on Fig. 8a).

continuity geometry in the gneiss of Western Norway is the occurrence of a joint set perpendicular to the dip line of the metamorphic foliation (although their origin is still poorly understood; e.g. Weinberger *et al.* 2010). At Børa, it would correspond to a flat-lying joint set as identified by Braathen *et al.* (2004). The development of the instability would be then better explained by a mechanism of sagging along such flat-lying discontinuities, accompanied by an opening along the vertical sets of discontinuities. As such, Børa is classified as a planar styled complex field (Braathen *et al.* 2004). The large-scale gravitational deformation at Børa would involve between 50 and 200 Mm^3 of rocks (Braathen *et al.* 2004). The uncertainty in the volume estimation is due to the unknown extent in depth of the instability. The volumes of local instabilities located at the edge of the plateau (Fig. 12c) are roughly estimated to be of approximately half a Mm^3.

Three of these local instabilities show displacement rates between 0.2 and 2 cm/yr based on periodic dGPS measurements (Fig. 12). No displacements are measured for the entire unstable rock slope at Børa indicating that the active deformation takes place at the frontal cliff leading to the creation of the mentioned localized instabilities.

MANNEN

The Mannen rock slope displays a widespread gravitational deformation and comprises a collapsing instability at the edge of the 1300 m elevated plateau (Fig. 13a). Abundant scars of previous failures of various sizes are observed at Mannen and two related large deposits are preserved on the valley floor (Fig. 2; Blikra *et al.* 2002). Minor rockfalls are reported every year since the site is studied from 2007.

Contrary to the three other localities in Romsdalen valley where gravitational instabilities are encountered in the dioritic–granitic gneiss basement unit of the valley, the Mannen rock slope instabilities developed in a singular high-grade metamorphic unit made of intensively folded alternating sillimanite-bearing dioritic and muscovite-sillimanite granitic gneisses, amphibolites and pegmatites (Fig. 2; Saintot *et al.* 2011a).

Figure 10. a) Map of the rock slope instabilities at Flatmark on a hillshaded DEM and location of the slope profiles shown in (b); note the deposits of large rock slope failures in the valley bottom that are assumed to be from Flatmark. b) Topographic profiles across the instabilities; yellow lines: basal limits with uncertain dip angles; blue lines: back-cracks with unknown depth; red dashed lines: attitude of the metamorphic foliation. c) Map of the slope gradient at Flatmark showing the moderately valley-dipping topographic surfaces.

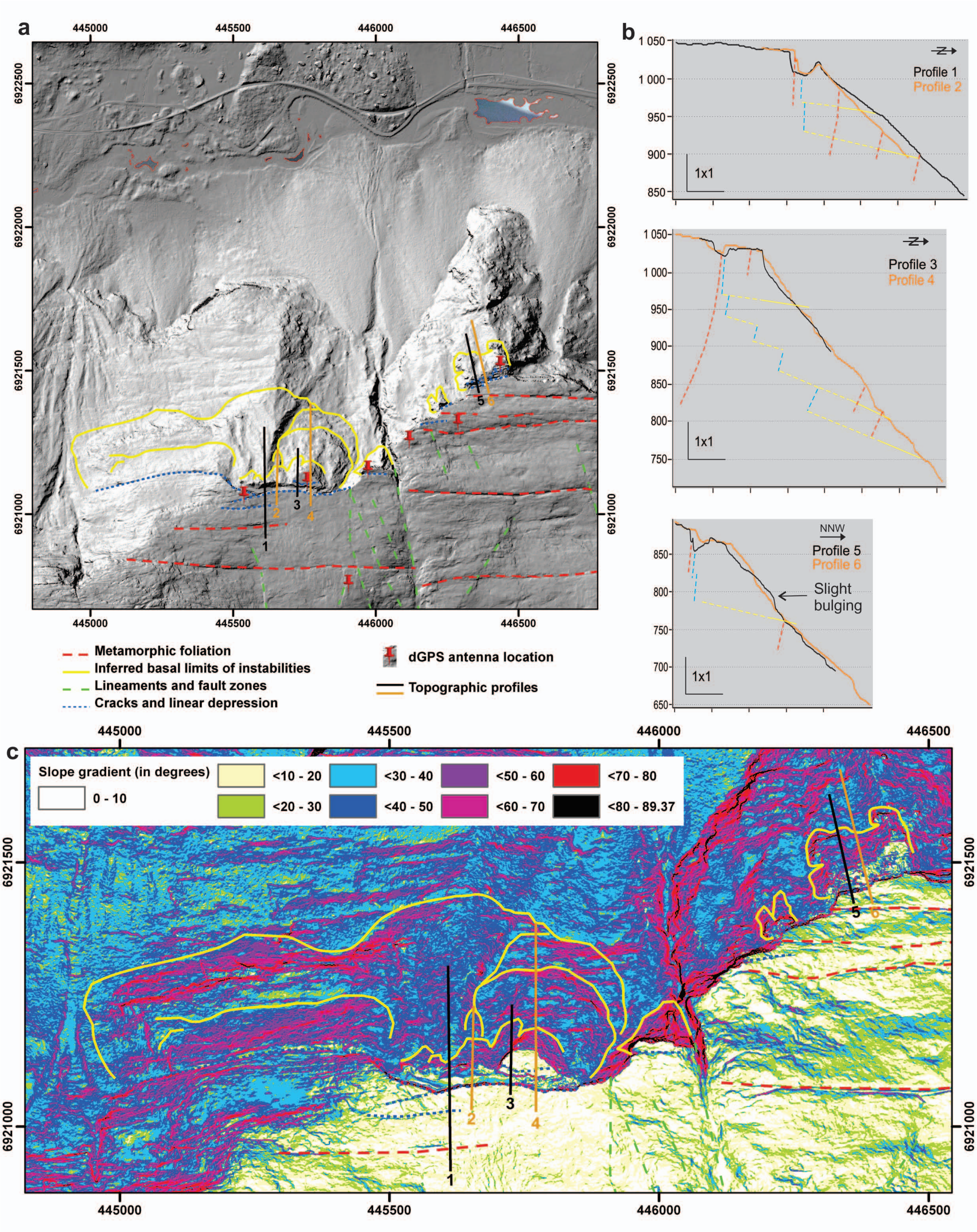
a
b
c
Metamorphic foliation
Inferred basal limits of instabilities
Lineaments and fault zones
Cracks and linear depression
dGPS antenna location
Topographic profiles
Profile 1
Profile 2
Profile 3
Profile 4
Profile 5
Profile 6
NNW
Slight bulging
1x1
Slope gradient (in degrees)
0 - 10
<10 - 20
<20 - 30
<30 - 40
<40 - 50
<50 - 60
<60 - 70
<70 - 80
<80 - 89.37

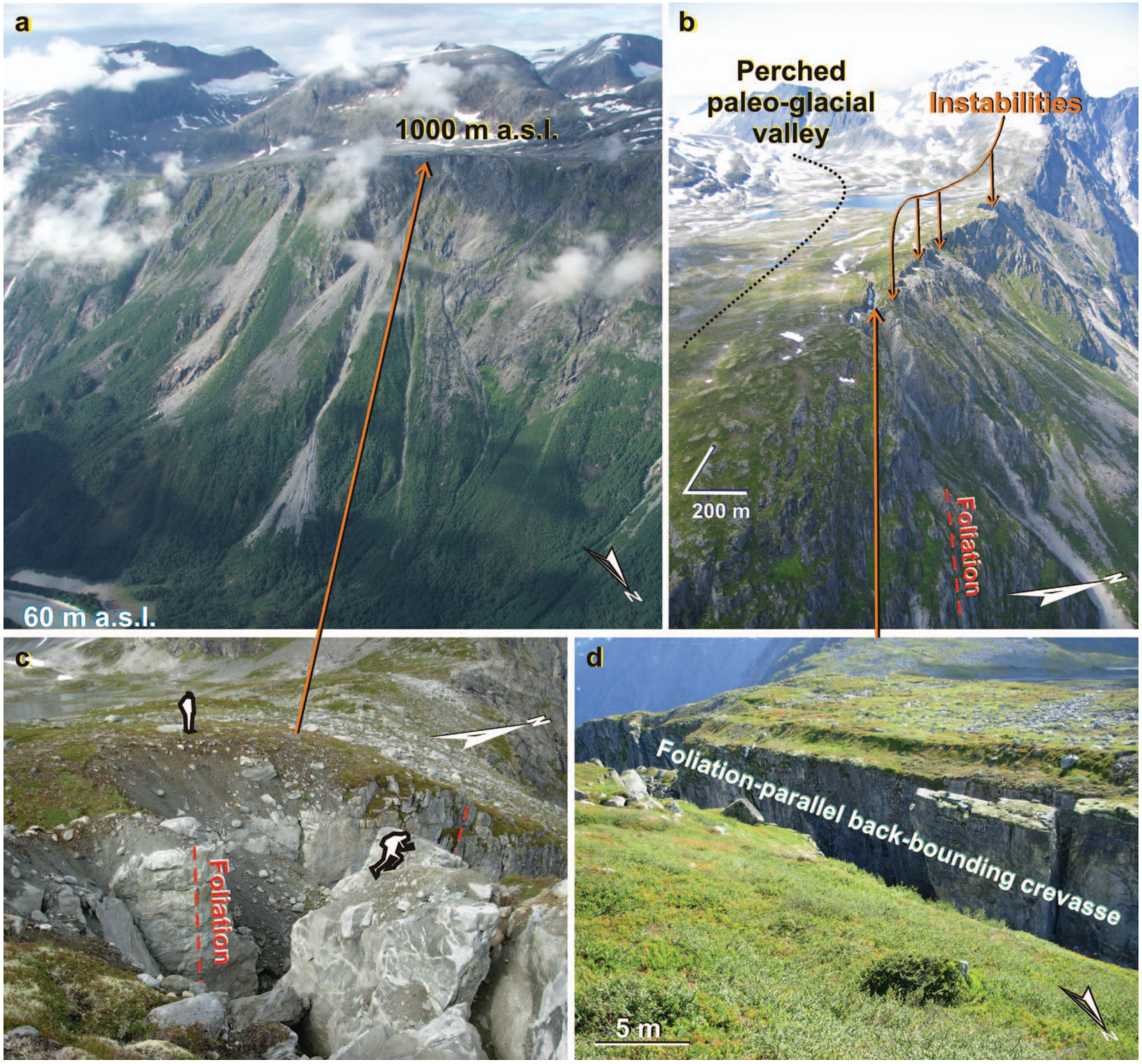

Figure 11.
a) Photograph of the Børa unstable rock slope (by courtesy of Tor Farsund) displaying the frequent rockfall events. b) Photograph of the perched paleo-glacial valley trending parallel to the cliff. The cliff is shaped by the steep metamorphic foliation planes. c) Photograph of one of the moving local instabilities at the edge of Børa plateau. d) The eastern end of the back-bounding crevasse of the gravitational deformation at Børa.

The field studies on the plateau behind the unstable rock slope has allowed recognizing widespread gravitational deformation by opening of the penetrative steep E-W metamorphic foliation and a set of nearly perpendicular vertical N-S/NNE-SSW fractures (Fig. 13a-c). The latter are copies of a regional tectonic fault displaying an epidote- and chlorite-rich fault core inherited from a ductile shear zone (Fig. 13a, d, e). This fault makes a clear boundary between the unstable parts of the slope in the east and the stable parts in the west (Fig. 13a, d).

The geomorphological DEM analysis coupled with aerial photographs has allowed defining the limits of the deformed rock slope. Three instabilities based upon different deformed volumes are retained (Dahle *et al.* 2008, 2010). The first volume corresponds to the moving upper part of the unstable rock slope and may reach a volume of 2–3.5 Mm^3 (Fig. 14a; Farsund 2011). Due to motion a topographic bulge is visible at its front (Fig. 14b). At the base of the instability a surface underlined by frequent rockfalls satisfies the geometry of a sliding surface (Fig. 14b). The continuation of this surface within the mountain intersects a vertical borehole that was drilled from the top of the unstable block (Fig. 14b) at c. 75 m depth. At this depth the drill core is formed by a c. 15 m thick zone of much damaged rocks, which comprises layers of crushed rocks, clay-rich gouges and fine-grained breccias (Saintot *et al.* 2011a).

However, the attitude of this sliding surface extracted from the ALS-DEM (dip direction/dip angle: N110/48°; Fig. 14c) is highly oblique to the slope and a planar failure along this surface only seems to be unlikely. With the help of the 3D model of the slope a second sliding surface (N023/59°) was identified permitting the development of a wedge sliding mechanism (Dahle *et al.* 2010; Farsund 2011). The intersection of these two sliding surfaces, i.e. the possible sliding direction, fits well with the displacement vectors determined by dGPS measurements that plunges of 50° toward N060-070 (Fig. 14c).

The unstable rock slope at Mannen has been classified as instability with high susceptibility for failure when a movement of 4-5 cm/year of the 2–3.5 Mm^3 instability at the edge of the plateau was detected by dGPS measurements (Dahle *et al.* 2008).

Because of the catastrophic consequence of a failure, this block is under continuous monitoring since 2009 and multi-disciplinary studies follow each other (Dahle *et al.* 2008, 2010, 2011, Saintot *et al.* 2011a). The second unstable volume includes the first volume and would reach 25–30 Mm^3 (Fig. 14a; Farsund 2011). Its basal limits are not clearly visible in the field or on the ALS-DEM or aerial photographs. A severely damaged zone identified along the drill core at 113–115 m depth might correspond to the basal failure surface of this second unstable volume (Saintot *et al.* 2011a). Its lateral and upper boundaries partly coincide with those of the first instability, but they are not underlined by signs of activity (openings, rockfall activity, etc.; Fig. 14a). Since the structural limits of this deformed volume are not accurately defined, its kinematics is not fully understood. Therefore, this second unstable volume is considered to have a lower susceptibility for failure than the first volume (Dahle *et al.* 2010).
The third potential instability encompasses the entire gravitationally deformed slope far inward the plateau and has a volume of 80–100 Mm^3 (Fig. 13a). The lateral and basal limits of this third instability are visible neither in the field, nor on the ALS-DEM and aerial photographs. In addition there are no ongoing displacements or other signs of activity and therefore is this third volume considered as stable (Dahle *et al.* 2010; Fig. 14a).

DISCUSSION WITH CONCLUSIVE REMARKS

The four sites of Svarttinden, Flatmark, Børa and Mannen display large gravitational deformation that evoke the normal process of slope denudation: the deformation occurs on knick-points of the slope and the total failure will smooth the slope to a steady state (Ahnert 1987, Selby 1993, Böhme *et al.* 2011).
The kinematic feasibility of failure is clearly determined for Svarttinden rockslide. It is a planar failure on an ideally 45° valley-dipping basal surface. However, it is noticed that the surface is rough and undulated and that, at the toe zone of the rockslide, its change in dip direction may act as a buttress to sliding.

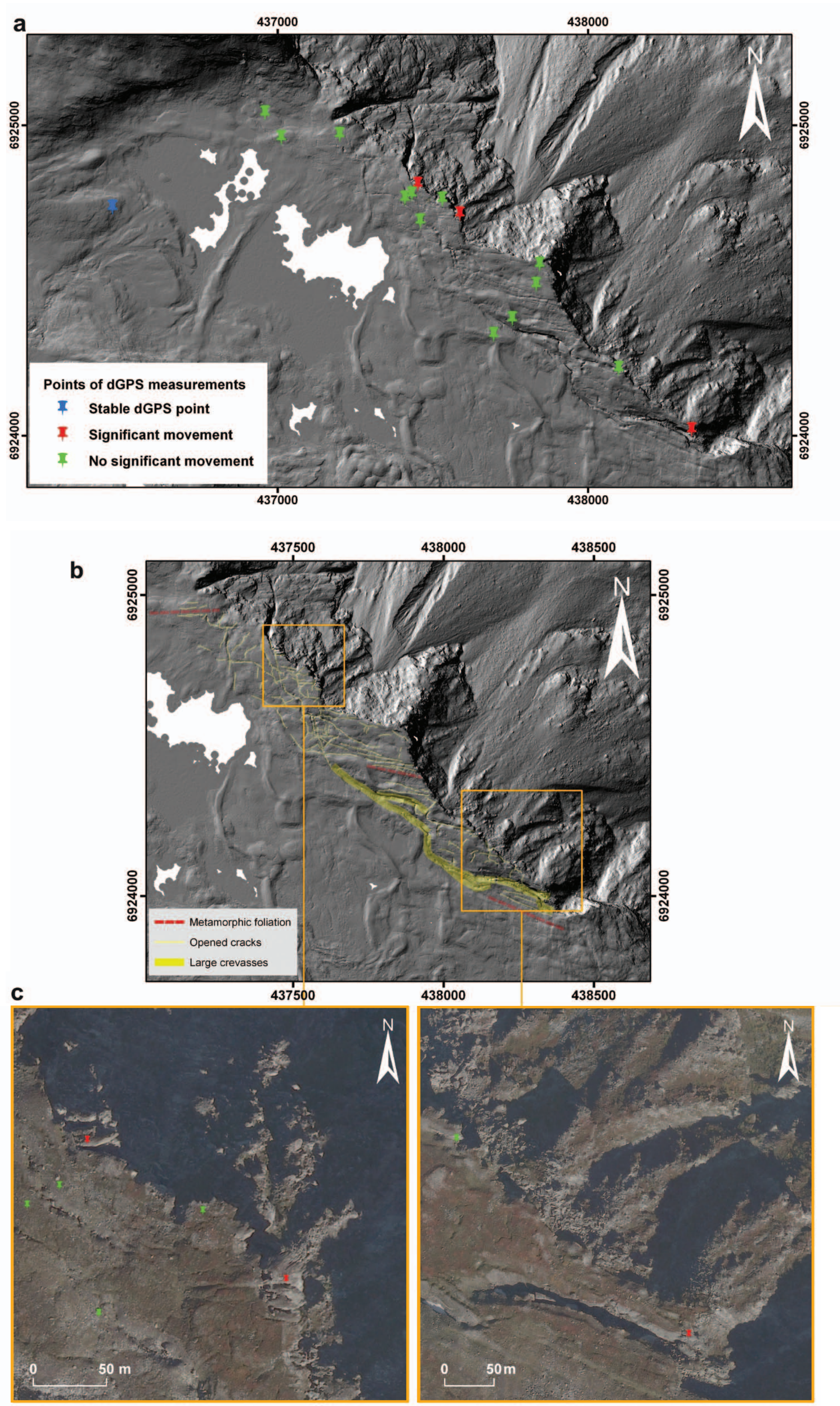

Figure 12. a) Hillshaded ALS-DEM of the Børa plateau with dGPS antenna positions and associated detection of movements. The movements are significant on 3 local instabilities at the edge of Børa plateau and range between 0.2 and 2 cm/yr. b) Structural map of the deformed edge of Børa plateau from the analysis of the ALS-DEM. c) And d) detailed aerial photographs of the three local instabilities.

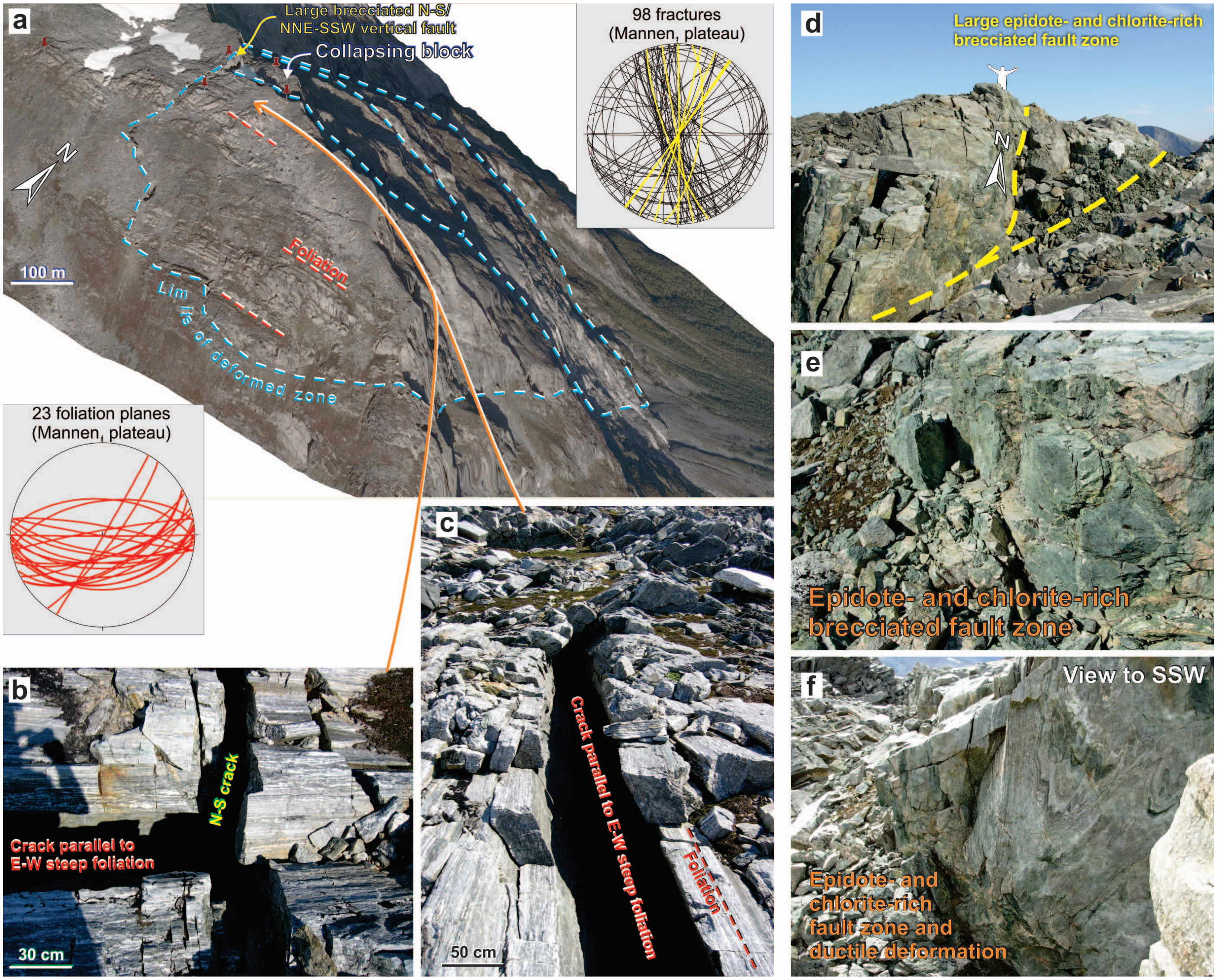

Figure 13. a) Aerial photograph draped on the ALS-DEM of the deformed edge of Mannen plateau (view from above) and stereonet of field data (in yellow, mineralized fracture surfaces); red pins mark the location of dGPS antennas. b) And c) photographs of E-W cracks and N-S cracks that respectively opened parallel to the steep metamorphic foliation and along N-S fractures. d) and e) A roughly N-S trending epidote-rich cataclastic fault limits the instability to the west. f) The epidote-rich cataclastic fault (shown in (d) and (e)) is also a pre-existing discrete zone of high ductile strain.

The failure mechanism at the edge of Flatmark and Børa plateau is less clearly understood. The only well developed and identifiable structures are the back-cracks, which largely follow the steep foliation surfaces and their opening by tension is indubitable. The involvement of such large slope volumes (several Mm^3) in the gravitational deformation would require deformation on basal surfaces rather than toppling, but no conspicuous basal sliding surfaces are detected so far at Flatmark and Børa. At Flatmark, shallow valley-dipping joints exist that may allow a sliding of the rock mass. At Børa, the joints would be flat-lying and a sagging of rock volumes at the edge of the plateau is the retained mechanism of deformation. In itself, the entire deformed volume at Børa typically resembles the complex fields that developed at edges of plateaus in Norway (Braathen *et al.* 2004, Böhme *et al.* 2011).

At the uppermost instability of Mannen, two basal surfaces identified through an analysis of the ALS-DEM form a wedge along which the sliding of the instability may occur. One of the basal surfaces is the locus of frequent rockfalls and may also fit with a thick zone of severely damaged rocks at c. 70-80 m depth identified in the borehole drilled from the top of the instability. Large tectonic fault zones when intersecting the slopes are prone to be reactivated under gravity. An epidote- and chlorite-rich cataclastic fault is the basal detachment of the Svarttinden rockslide. At Flatmark and Mannen, large cataclastic vertical faults are the lateral limits of the instabilities. At Mannen and Svarttinden, these prominent brittle structures were also the locus of high ductile strain. Such discontinuities have a protracted geological history and are likely zones of weakness within the hard gneissic rocks of Romsdalen valley.

As already mentioned, Mannen is located in a specific rock unit of the basement that comprises a range of petrology and displays an intense ductile deformation (with disharmonic and recumbent close to tight folds being common). The conspicuous difference in the bedrock at Mannen and in its structural pattern might partly explain the large finite gravitational deformation of Mannen slope and its subsequent present-day state of high activity (Henderson and Saintot 2007, Dahle *et al.* 2008). It is a qualitative assessment which aims at explaining the specific case of Mannen based on the rheological contrast of the bedrocks along the southern side of the Romsdalen valley.

While the local instabilities at Børa are susceptible for failure, the large deformed area inward the plateau is not. However, it cannot be ruled out that a very low, not detectable, rate of opening of the back-bounding crevasse may have very important effect on the free border of the rock volume, i.e. on the highly unstable structures at the edge of the plateau. The comparison with the site of Flatmark, where no large gravitational structures developed inward the plateau and no displacement are recorded on the instabilities at the edge of the plateau, lets envisage that a link exists between the occurrence of widespread gravitational deformation affecting the Børa plateau far from its edge and the present movements of local instabilities at the edge. Further investigations are required to better understand this possible link, even though the imbrications of localized, small instabilities within large gravitational slope deformations are quite common (e.g. Agliardi *et al.* 2001, Ambrosi and Crosta 2006).

A conceptual model to explain the large-scale gravitational deformation at Børa involving maybe more than 200 Mm^3 of rocks considers the presence of a paleoglacial valley trending parallel to the cliff (and which may actually be the only geomor-

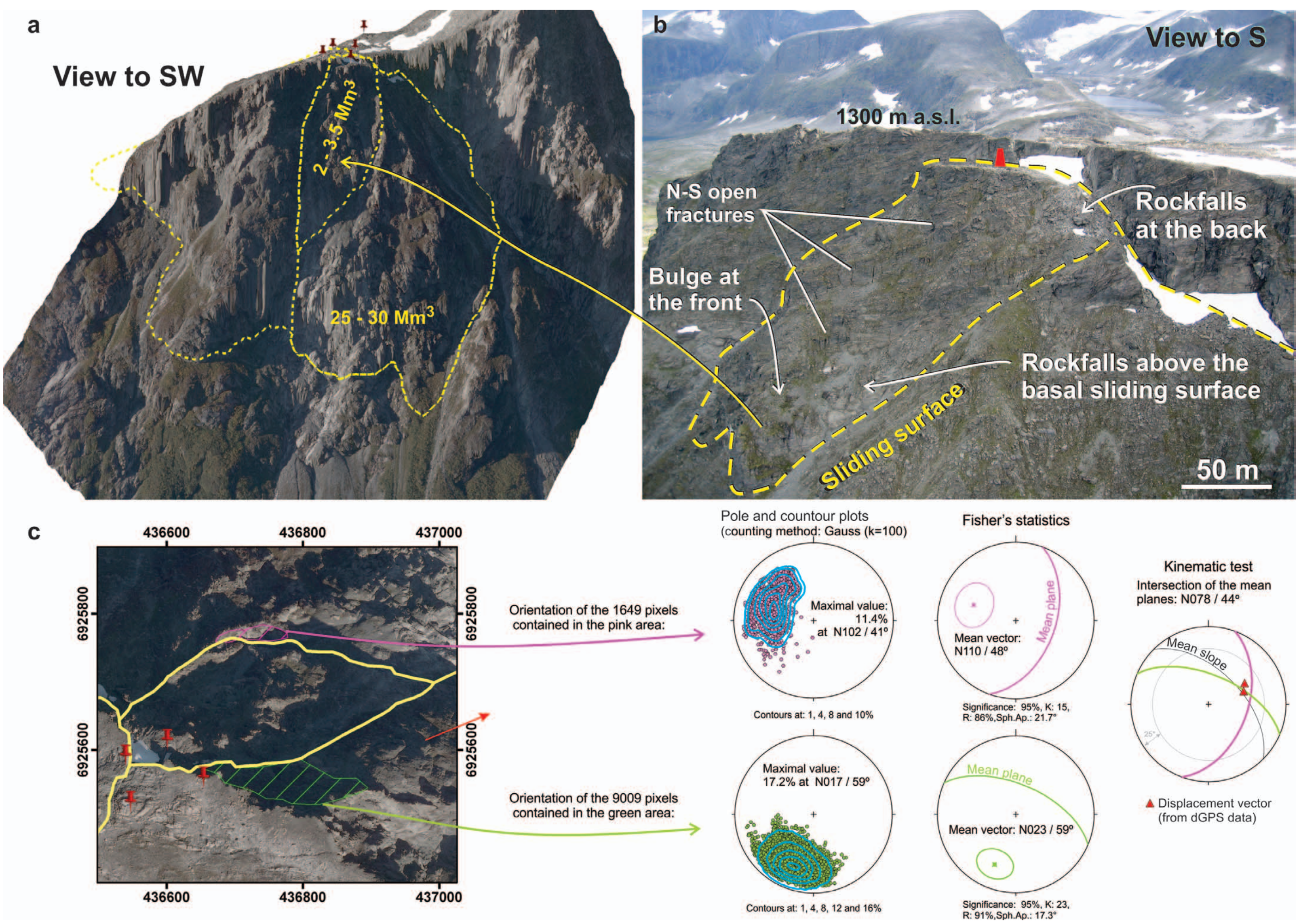

Figure 14. a) Aerial photograph draped on the ALS-DEM of the Mannen rock slope. Yellow lines: inferred limits of the instabilities; red pins: location of the dGPS antennas. b) Photograph from helicopter of the uppermost instability at Mannen with an important set of N-S trending opened fractures, a bulge at the front and a sliding surface underlined by rockfall events. The red cone marks the location of the drilling site. c) Determination of a wedge sliding mechanism on two outcropping surfaces at the limit of the uppermost instability at Mannen. The mean planes matching the mean orientations of these surfaces are extracted from the ALS-DEM and the wedge intersection line fits well with the displacement vector obtained from dGPS measurements.

phological difference with Flatmark area). Assumption is made that, at the base of the glacier, the vertical foliation would have weaken either by opening of these vertical planes by ice loading or by weathering of mica-rich foliation layers due to water circulation or both (e.g. Saintot *et al.* 2011b). It is also noticeable that the finite deformation along the km long bounding crevasse appears to have been larger eastward, where the paleoglacial valley intersects the edge of the plateau toward the Romsdal valley. The question is opened if more flowing water at this location and thus more weathering could have favored more deformation later on (e.g. Bachmann *et al.* 2004).

The large potential rock slope instabilities presented in this contribution are on the southern side of Romsdalen valley. No such large gravitational instability is nowadays observed on the northern slope of the Romsdalen valley, while some scars and deposits of previous large events are visible. The detailed geometrical characterization of these scars is expected to reveal parameters that may count for the difference of behavior of the two slopes of the Romsdalen valley. As the field study is avoid due to the steepness of the slopes, this will be mainly based on the analyses of the ALS-DEM and of its derivatives.

The four unstable rock slopes may be ranked in terms of susceptibility for failure. The uppermost instability at Mannen has without any doubt the highest susceptibility for failure with 5 decisive parameters: (1) velocity of the moving block of 4-5 cm/year, (2) rockfall activity along the sliding surface, (3) bulging of the topography at its front, (4) structures that kinematically explain the failure and (5) weak layers along the probable basal failure surface. The 3 local instabilities at the edge of Børa plateau have medium to high susceptibility for failure with velocities of 0.2-2 cm/yr and frequent rockfall activity, even though the failure mechanisms are not fully understood. The Svarttinden rockslide is structurally well defined and displays indications of past displacements with a well-developed frictional product along its single basal sliding surface. East of the remaining instability, a large volume already failed along the same basal sliding surface. However, there are no sign of current displacement of the instability and rockfalls are restrained to its very steep faces, which cannot be interpreted as sign of activity for the rock slope instability. Therefore, the Svarttinden rock slope instability has a medium susceptibility for failure. The instabilities at Flatmark are well detached from the edge of the plateau but no conspicuous activity is observed from the deformed slope. Thus, the rock slope instabilities at Flatmark are considered having a low susceptibility for failure. The instabilities at Svarttinden and Flatmark are nonetheless under periodic monitoring because of the severe consequences of a catastrophic failure. Repetitive TLS surveys are performed in the aim to supplement the dGPS method in the detection of eventual displacements. Any increase in displacements or other signs of activity will lead to a reassessment and likely to an increase of the susceptibility for failure of these instabilities.

The present study strengthens the importance of a geological understanding of the rock slope deformation. The detailed structural analysis of gravitational rock slope instabilities leads to accurately carry out the kinematic feasibility of failure. It is also a necessary step for further advanced studies. Among other possibilities, it may allow the construction of geometrically correct numerical modeling on slope stability including the implementation of the discontinuity sets and the good localization of the borders of the deformed rock mass. The latter leads to a good estimation of the unstable volumes used to assess propagation scenarios.

ACKNOWLEDGEMENTS

The authors thank the Norwegian Water and Energy Resources Directorate for funding this study through the national plan for mapping unstable rock slopes. M. Jaboyedoff and R. Hermanns are kindly acknowledged for their review. This work is International Centre for Geohazards (ICG) contribution No. 382.

LIST OF REFERENCES

Agliardi, F., Crosta, G. B. y Zanchi, A. 2001. Structural constraints on deep-seated slope deformation kinematics. Engineering Geology 59: 83-102.

Ahnert, F. 1987. Process-response models of denudation at different spatial scales. Catena Supplement 10: 31-50.

Ambrosi, C. y Crosta, G.B. 2006. Large sackung along major tectonic features in the central Italian Alps. Engineering Geology 83: 183-200.

Bachmann, D., Bouissou, S. y Chemenda, A. 2004. Influence of weathering and pre-existing large scale fractures on gravitational slope failure: insights from 3-D physical modeling. Natural Hazards and Earth System Sciences 4: 711-717.

Böhme, M., Saintot, A., Henderson, I., Henriksen, H. y Hermanns, R.L. 2011. Slope instabilities in Sogn og Fjordane County, Norway. In Jaboyedoff, M. (ed.) Slope Tectonics, Geological Society, London, Special Publications 351: 97-111.

Blikra, L.H., Braathen, A., Anda, E., Stalsberg, K. y Longva, O. 2002. Rock avalanches, gravitational bedrock fractures and neotectonic faults onshore northern Norway: Examples, regional distribution and triggering mechanisms. NGU Report 2002.016, Geological Survey of Norway, Trondheim, Norway.

Blikra, L.H., Longva, O., Braathen, A., Anda, E., Dehls, J. y Stalsberg, K. 2006. Rock slope failures in Norwegian fjord areas: examples, spatial distribution and temporal pattern. In Evans, S.G., Scarascia Mugnozza, G., Strom, A. y Hermanns, R.L. (eds.) Landslides from Massive Rock Slope Failure, NATO Science Series, IV. Earth and Environmental Sciences 49, Springer: 475-496, Dordrecht, Netherlands.

Braathen, A., Blikra, L.H., Berg, S.S. y Karlsen, F. 2004. Rock slope failures in Norway; type, geometry, deformation mechanisms and stability. Norwegian Journal of Geology 84: 67-88.

Brideau, M.-A., Stead, D., Kinakin, D. y Fecova, K. 2005. Influence of tectonic structures on the Hope Slide, British Columbia, Canada. Engineering Geology 80: 342-359.

Brideau, M.-A., Yan, M. y Stead, D. 2009. The role of tectonic damage and brittle rock fracture in the development of large rock slope failures. Geomorphology 103: 30-49.

Cruden, D.M. 1976. Major slides in the Rockies. Canadian Geotechnical Journal 13: 8-20.

Cruden, D.M. y Varnes, D.J. 1996. Landslide types and processes. In Turner, A.K. and Schuster, R.L. (eds.) Landslides: Investigation and Mitigation. Special Report 247, Transportation Research Board, National Research Council, Washington DC: 36-75.

Dahle, H., Anda, E., Saintot, A. y Sætre, S. 2008. Faren for fjellskred fra fjellet Mannen i Romsdalen. NGU Report 2008.087, Geological Survey of Norway, Trondheim, Norway [in Norwegian].

Dahle, H., Saintot, A., Blikra, L.H. y Anda, E. 2010. Geofagleg oppfølging av ustabilt fjellparti ved Mannen i Romsdalen. NGU Report 2010.022, Geological Survey of Norway, Trondheim, Norway [in Norwegian].

Dahle, H., Bjerke, P.L., Crosta, G., Hermanns, R.L., Anda, E. y Saintot, A. 2011. Faresoner for utløp, oppdemming og flom som følge av fjellskredfare ved Mannen, NGU Report 2011.058, Geological Survey of Norway, Trondheim, Norway [in Norwegian].

Eberhardt, E., Stead, D. y Coggan, J.S. 2004. Numerical analysis of initiation and progressive failure in natural rock slopes – the 1991 Randa Rockslide. International Journal of Rock Mechanics and Mining Sciences 41: 69-87.

El Bedoui, S., Guglielmi, Y., Lebourg, T. y Pérez, J.-L. 2008. Deep-seated failure propagation in a fractured rock slope over 10,000 years: the La Clapière slope, the south-eastern French Alps. Geomorphology 105: 232-238.

ESRI (Environmental Systems Research Institute) 2010. ArcGIS [software]. Version 10, Environmental Systems Research Institute Inc., Redlands, CA.

Etzelmüller, B., Romstad, B. y Fjellanger, J. 2007. Automatic regional classification of topography in Norway. Norwegian Journal of Geology 87: 167-180.

Farsund, T.Ø. 2010. Geology, DEM analysis and geohazard assessment of the Romsdalen valley. Unpublished MSc project thesis TGB4500, Department of geology and mineral resources engineering, Norwegian University of Sciences and Technology, Trondheim.

Farsund, T.Ø. 2011 Geological and numerical stability modelling of Mannen, Romsdalen MSc thesis in Petroleum Geosciences and Engineering, Norwegian University of Sciences and Technology, Trondheim.

Fell, R., Corominas, J., Bonnard, C., Cascini, L., Leroi, E. y Savage, W.Z. 2008. Guidelines for landslide susceptibility, hazard and risk zoning for land use planning. Engineering Geology 102: 85-98.

Fisher, R.A. 1953. Dispersion on a sphere. Proceedings of the Royal Society of London, Series A, 217: 295–305.

Ganerød, G.V., Grøneng, G., Rønning, J.S., Dalsegg, E., Elvebakk, H., Tønnesen, J.F., Kveldsvik, V., Eiken, T., Blikra, L.H. y Braathen, A. 2008. Geological model of the Åknes rockslide, western Norway. Engineering Geology 102: 1-18.

Giraud, A., Rochet, R. y Antoine, P. 1990. Processes of slope failure in crystallophyllian formations. Engineering Geology 29: 241-253.

Guzzetti, F., Cardinali, M. y Reichenbach, P. 1996. The influence of tectonic setting and lithology on the landslide type and pattern. Environmental and Engineering Geoscience 2: 531-555.

Henderson, I.H.C. y Saintot, A. 2007. Fjellskredundersøkelser i Møre og Romsdal. NGU Report 2007.043, Geological Survey of Norway, Trondheim, Norway [in Norwegian].

Henderson, I.H.C., Saintot, A. y Derron, M.-H. 2006. Structural mapping of potential rockslide sites in the Storfjorden area, Western Norway: the influence of bedrock geology on hazard analysis. NGU Report 2006.052, Geological Survey of Norway, Trondheim, Norway.

Henderson, I.H.C. y Saintot, A. 2011. Regional spatial variations in rockslide distribution from structural geology ranking: an example from Storfjorden, western Norway. In Jaboyedoff, M. (ed.) Slope Tectonics. Geological Society Special Publication 351, p. 79.

Hermanns, R.L. y Strecker, M.R. 1999. Structural and lithological controls on large Quaternary rock avalanches (sturzstroms) in arid northwestern Argentina. Geological Society of America Bulletin 111: 934-948.

Hoek, E. y Bray, J. 1981. Rock slope engineering, revised 3rd edition. The Institution of Mining and Metallurgy, London: 37-63.

Hossack, J.R. y Cooper, M.A. 1986. Collision tectonics in the Scandinavian Caledonides. Geological Society of London. Special Publication 19: 287-304.

InnovMetric 2012. PolyWorks: 3D scanner and 3D digitizer software from InnovMetric Software Inc. http://www.innovmetric.com/polyworks/3D-scanners/home.aspx?lang=en, accessed 20.01.2012.

Jaboyedoff, M., Baillifard, F., Couture, R., Locat, J. y Locat, P. 2004a. New insight of geomorphology and landslide prone area detection using Digital Elevation Model(s). In Lacerda, W.A., Ehrlich, M., Fontoura, A.B. y Sayão, A. (eds.) Landslides: Evaluation and Stabilization, Taylor & Francis Group: 191-198, London.

Jaboyedoff, M., Baillifard, F., Couture, R., Locat, J. y Locat, P. 2004b. Toward preliminary hazard assessment using DEM topographic analysis and simple mechanical modeling by means of sloping local base level. In Lacerda, W.A., Ehrlich, M., Fontoura, A.B. and Sayão, A. (eds.) Landslides: Evaluation and Stabilization, Taylor & Francis Group: 199-205, London.

Jaboyedoff, M., Couture, R. y Locat, P. 2009. Structural analysis of Turtle Mountain (Alberta) using digital elevation model: Towards a progressive failure. Geomorphology 103: 5-16.

Jaboyedoff, M., Oppikofer, T., Derron, M.-H., Blikra, L.H., Böhme, M. y Saintot, A. 2011. Complex landslide behaviour and structural control: a three dimensional conceptual model of the Åknes rockslide, Norway. In Jaboyedoff, M. (ed.) Slope Tectonics, Geological Society, London, Special Publications 351: 147-162.

Julian, M. y Anthony, E. 1996. Aspects of landslide activity in the Mercantour Massif and the French Riviera, southeastern France. Geomorphology 15: 275-289.

Kellogg, K.S. 2001. Tectonic controls on a large landslide complex: Williams Fork Mountains near Dillon, Colorado. Geomorphology 41: 355-368.

Longchamp, C., Delasoie, F., Carrea, D., Derron, M.-H., Oppikofer, T. y Jaboyedoff, M. 2010. Analysis of groundbased Lidar data from Møre og Romsdal County (Norway), Unpublished Report IGAR – UNIL.

Longva, O., Blikra, L.H. y Dehls, J. 2009. Rock avalanches – distribution and frequencies in the inner part of Storfjorden, Møre og Romsdal County, Norway. NGU report 2009.002, Geological Survey of Norway, Trondheim, Norway.

Mahr, T. 1977. Deep-reaching gravitational deformations of high mountain slopes. Bulletin of the International Association of Engineering Geology 16: 121-127.

Mangerud, J. 2004. Ice sheet limits in Norway and on the Norwegian continental shelf. In Ehlers, J. y Gibbard, P.L. (eds.) Quaternary Glaciations Extent and Chronology Part I: Europe, Elsevier: 271-294.

Mosar, J. 2003. Scandinavia's North Atlantic passive margin. Journal of Geophysical Research 108: NO. B8, 2360, doi:10.1029/2002JB002134.

Olesen, O., Dehls, J., Bungum, H., Riis, F., Hicks, E., Lindholm, C., Blikra, L.H., Fjeldskaar, W., Olsen, L., Longva, O., Faleide, J.I., Bockmann, L., Rise, L., Roberts, D., Braathen, A. y Brekke, H. 2000. Neotectonics in Norway, Final Report. Geological Survey of Norway, Report 2000.002, Geological Survey of Norway, Trondheim, Norway.

Olesen, O., Blikra, L.H., Braathen, A., Dehls, J.F., Olsen, L., Rise, L., Roberts, D., Riis, F., Faleide, J.I. y Anda, E. 2004. Neotectonic deformation in Norway and its implications: a review. Norwegian Journal of Geology 84: 3-34.

Oppikofer, T. 2009. Detection, analysis and monitoring of slope movements by high resolution digital elevation models, PhD thesis, Institute of Geomatics and Analysis of Risk, University of Lausanne, Lausanne, Switzerland.

Oppikofer, T., Jaboyedoff, M., Blikra, L.H. y Derron, M.-H. 2009. Characterization and monitoring of the Åknes rockslide using terrestrial laser scanning. Natural Hazards and Earth System Sciences 9: 1003-1019.

Oppikofer, T., Jaboyedoff, M., Pedrazzini, A., Derron, M.-H. y Blikra, L.H. 2011. Detailed DEM analysis of a rockslide scar to improve the basal failure surface model of active rockslides. Journal of Geophysical Research 116: F02016. doi:10.1029/2010JF001807.

Oppikofer, T., Hermanns, R.L., Redfield, T.F., Sepúlveda, S.A., Duhart, P. y Bascuñan, I. 2012. Morphologic description of the Punta Cola rock avalanche and associated minor rockslides caused by the 21 April 2007 Aysén earthquake (Patagonia, southern Chile). Revista de la Asociación Geológica Argentina, this volume.

Pedrazzini, A., Froese, C.R., Jaboyedoff, M., Hungr, O. y Humair, F. 2012. Combining digital elevation model analysis and run-out modelling to characterize hazard posed by a potentially unstable rock slope at Turtle Mountain, Alberta, Canada. Engineering Geology DOI:10.1016/j.enggeo.2011.03.015.

Roberts, D. 2003. The Scandinavian Caledonides: event chronology, palaeogeographic settings and likely modern analogues. Tectonophysics 363: 283-299.

Roberts, D. y Gee, D.G. 1985. An introduction to the structure of the Scandinavian Caledonides. In Gee, D.G. and Sturt B.A. (eds) The Caledonide Orogen - Scandinavia and related areas 55-68. John Wiley and Sons, Chichester.

Saintot, A., Elvebakk, H., Ganerød, G.V., Oppikofer, T. y Farsund, T. 2011a. Mannen unstable rock slope (Romsdal, Møre & Romsdal County): Logging of drill hole and core KH-01-10, geomorphological interpretation of a 1 m resolution digital elevation model and terrestrial laser scan displacement analysis. NGU Report 2011.026, Geological Survey of Norway, Trondheim, Norway.

Saintot, A., Henderson, I. y Derron, M.-H. 2011b. Inheritance of ductile and brittle structures in the development of large rock slope instabilities: examples from Western Norway. In Jaboyedoff, M. (ed.) Slope Tectonics, Geological Society, London, Special Publications 351: 27-78.

Sauchyn, D.J., Cruden, D.M. y Hu, H.Q. 1998. Structural control of the morphometry of open rock basins, Kananaskis region, southwestern Alberta. Geomorphology 22: 313–324.

Selby, M.J. 1993. Hillslope Materials and Processes. Oxford University Press, New York.

Skrednett 2012. Skreddata på nett. http://www.ngu.no/kart/skrednett, accessed 06.02.2012 [in Norwegian].

Torsvik, T.H., Andersen, T.B. Eide, E.A. y Walderhaug, H.J. 1997. The age and tectonic significance of dolerite dykes in western Norway. Journal of Geological Society of London 154: 961-973.

Tveten, E., Lutro, O. y Thorsnes, T. 1998. Geologisk kart over Norge, berggrunnskart Ålesund, 1:250,000. Geological Survey of Norway, Trondheim [in Norwegian].

Valle, P., Faerseth, R. B. y Fossen, H. 2002. Devonian–Triassic brittle deformation based on dyke geometry and fault kinematics in the Sunnhordland region, SW Norway. Norwegian Journal of Geology 82: 3-17.

Varnes, D.J. 1978. Slope movement types and processes. In Schuster, R.L. and Krizek, R.J. (eds.) Landslides, Analysis and Control. Transportation Research Board Special Report, 176. National Research Council, Washington, DC: 11-33.

Wallbrecher, E. 1986. Tektonische und gefügeanalytische Arbeitsweisen. Enke-Verlag, Stuttgart [in German].

Weinberger, R., Eyal, Y. y Mortimer, N. 2010. Formation of systematic joints in metamorphic rocks due to release of residual elastic strain energy, Otago Schist, New Zealand. Journal of Structural Geology 32: 288-305.

Welkner, D., Eberhardt, E. y Hermanns, R.L. 2010. Hazard investigation of the Portillo Rock Avalanche site, central Andes, Chile, using an integrated field mapping and numerical modelling approach. Engineering Geology 114: 278-297.

Recibido: 11 de febrero, 2012
Aceptado: 23 de abril, 2012